



6-1966

A pulse generator with a temperature-dependent pulse spacing.

Terry Dean Douglass
University of Tennessee

Follow this and additional works at: https://trace.tennessee.edu/utk_gradthes

Recommended Citation

Douglass, Terry Dean, "A pulse generator with a temperature-dependent pulse spacing.. " Master's Thesis, University of Tennessee, 1966.
https://trace.tennessee.edu/utk_gradthes/5786

This Thesis is brought to you for free and open access by the Graduate School at TRACE: Tennessee Research and Creative Exchange. It has been accepted for inclusion in Masters Theses by an authorized administrator of TRACE: Tennessee Research and Creative Exchange. For more information, please contact trace@utk.edu.

To the Graduate Council:

I am submitting herewith a thesis written by Terry Dean Douglass entitled "A pulse generator with a temperature-dependent pulse spacing.." I have examined the final electronic copy of this thesis for form and content and recommend that it be accepted in partial fulfillment of the requirements for the degree of Master of Science, with a major in Electrical Engineering.

J. F. Pierce, Major Professor

We have read this thesis and recommend its acceptance:

Accepted for the Council:

Carolyn R. Hodges

Vice Provost and Dean of the Graduate School

(Original signatures are on file with official student records.)

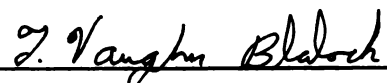
May 14 ,1966

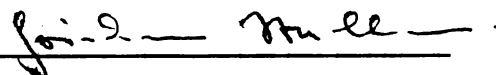
To the Graduate Council:

I am submitting herewith a thesis written by Terry Dean Douglass entitled "A Pulse Generator With a Temperature-Dependent Pulse Spacing." I recommend that it be accepted for nine quarter hours of credit in partial fulfillment of the requirements for the degree of Master of Science, with a major in Electrical Engineering.


Major Professor

We have read this thesis and
recommend its acceptance:





Accepted for the Council:


Dean of the Graduate School

A PULSE GENERATOR WITH A TEMPERATURE-DEPENDENT
PULSE SPACING

A Thesis
Presented to
the Graduate Council of
The University of Tennessee

In Partial Fulfillment
of the Requirements for the Degree
Master of Science

by
Terry Dean Douglass
June 1966

ACKNOWLEDGEMENTS

The author is sincerely grateful to Dr. J. F. Pierce whose suggestions led to the topic of this thesis and who provided the incentive and guidance during the preparation of this thesis. In addition, the author wishes to thank the Instrumentation and Controls Division, Oak Ridge National Laboratory, for its support in providing equipment for the experimental work and for its financial support in the preparation of the thesis. The author also wishes to express his gratitude to the National Science Foundation for the financial support through its Co-operative Graduate Fellowship program.

TABLE OF CONTENTS

CHAPTER	PAGE
I. INTRODUCTION	1
II. OPERATION OF A COLLECTOR-BASE ASTABLE MULTIVIBRATOR . . .	4
III. VARIABLES IN THE PULSE-WIDTH EQUATION	16
IV. VARIATIONS IN OUTPUT WAVEFORMS	20
V. A TEMPERATURE COMPENSATED AND STABILIZED CIRCUIT	24
VI. ANALYSIS OF PULSE SPACING WITH R_{B2} AS THE VARIABLE	29
VII. ANALYSIS OF THE OUTPUT SIGNAL WITH A CURRENT SOURCE AS A REPLACEMENT FOR R_{B2}	34
VIII. SUMMARY	45
LIST OF REFERENCES	48
APPENDIX	50

LIST OF FIGURES

FIGURE	PAGE
1. Circuit Diagram of a Transistor Astable Multivibrator . . .	5
2. Circuit Model of a Transistor Astable Multivibrator with Q_1 Saturated and Q_2 Nonconducting	7
3. Voltage Waveforms at the Base and Collector of Each Transistor as a Function of Time	10
4. Circuit Diagram of a Temperature Compensated and Stabilized Astable Multivibrator	26
5. Pulse Spacing as a Function of R_{B2}	30
6. Pulse Spacing as a Function of the Temperature of R_{B2} . . .	32
7. Pulse Spacing as a Function of Circuit Temperature	33
8. Circuit Model of a Transistor Astable Multivibrator with Q_1 Saturated and Q_2 Nonconducting with a Current Source as a Replacement for R_{B2}	35
9. Circuit Diagram of an Astable Multivibrator Using a Current Source for R_{B2}	38
10. Pulse Spacing as a Function of the Collector Current of the Current Source	39
11. Pulse Spacing as a Function of Diode Temperature	40
12. Circuit Diagram of an Astable Multivibrator Using a Linear Temperature-Dependent Current Source	41
13. The Inverse of Pulse Spacing as a Function of Transistor Temperature	44

CHAPTER I

INTRODUCTION

Multivibrators are closed-loop, positive-feedback systems having clearly defined stable or quasi-stable states. The nature of the states of such systems further categorizes multivibrators into three types: (1) astable multivibrators which have two quasi-stable states, (2) monostable multivibrators which have one quasi-stable state and one stable state, and (3) bistable multivibrators which have two stable states. Each type of multivibrator produces a signal form unique to its type. The astable multivibrator produces a rectangular wave signal that is self-starting and free-running. The monostable multivibrator produces a rectangular pulse signal that is triggered externally for each pulse. The bistable multivibrator switches from one state to another by external triggering for each state.

Basically the astable multivibrator is a signal-generating device. The rectangular waves generated have periods that are functions of the time required to switch from one quasi-stable state to another and back. These periods are dependent on the type of circuit, the parameters of the active devices, and the values of the circuit elements. If transistors are used as the active devices, the signal becomes a function of temperature since transistor parameters are temperature dependent. Also, the circuit elements are temperature dependent. The purpose of this study was to determine the possibilities of generating

a digital signal with an astable multivibrator circuit that was linearly dependent on temperature.

If the rectangular signal produced by the multivibrator is linearly dependent on temperature, the multivibrator can be classified as a linear temperature-to-digital signal converter. This type of converter would be very useful in any situation where a digital measurement of temperature is more advantageous than an analog measurement. For example, a digital signal is evidently more useful than an analog signal in digital computer applications. Also, an analog signal must be converted to a time-varying signal if it is to be used in telemetry situations. However, the digital signal generated by the multivibrator can be transmitted without any conversion. In addition, a digital signal is more advantageous than an analog signal in any high-interference condition. Thus, there are many uses for a rectangular wave generator that is linearly dependent on temperature.

The approximate expressions for the periods of the collector-base astable multivibrator indicated a linear relationship between the time periods of the rectangular wave and four of the circuit elements. Therefore, this circuit was chosen for this study. In Chapter II, expressions relating the time periods with the circuit and transistor parameters were developed. Millman and Taub (1)* present a very good but somewhat different analysis which includes the same parameters as

* Numbers in parentheses represent similarly numbered entries in the "List of References."

the analysis in Chapter II. Also in Chapter II, four of the limitations on the circuit elements and parameters were determined. The variables in the expressions relating the time periods with the circuit and transistor parameters were examined and evaluated in Chapter III. In Chapter IV, the variation in the signal waveform for a variation of both time periods was examined. From this examination the most desirable signal waveform was determined.

To make the output signal independent of temperature except for the temperature-dependent element, the remainder of the circuit was temperature compensated or stabilized. This temperature compensation and stabilization was developed in Chapter V. In Chapter VI, the results obtained by using a sensing resistor as the temperature-variable element were discussed. As a useful modification of the original astable multivibrator, the sensing resistor was replaced by a constant current source. In this case, a linear relationship was obtained between the inverse of the time period and the current of the current source. The analysis of this modified circuit and the presentation of experimental results were included in Chapter VII. In all cases where applicable, the theoretical and experimental results were compared.

CHAPTER II

OPERATION OF A COLLECTOR-BASE ASTABLE MULTIVIBRATOR

The circuit diagram of a collector-base astable multivibrator with quasi-stable transistor states of cutoff and saturation is shown in Figure 1. If the proper circuit values are used, Q_1 switches from cutoff to saturation, and Q_2 correspondingly switches from saturation to cutoff. The objective of this section is to determine expressions for the time periods of each of the quasi-stable states. Also, in this section some restrictions on the circuit values and transistor parameters are determined. The procedure in obtaining these objectives is to write circuit equations for a circuit model when one of the transistors is saturated and the other transistor is nonconducting. From these equations the quasi-stable periods are found and the voltage waveforms are determined. From the voltage waveforms and from the requirement of saturation, four important circuit element and transistor restrictions are found.

Analysis of the circuit depicted by Figure 1 begins by assuming that at $t = 0^-$ Q_1 is nonconducting and Q_2 is saturated. At $t = 0$, assume that the voltage on C_2 has reached the value where Q_1 becomes conducting. With Q_1 conducting, the current through R_{C1} increases, which decreases the collector-to-emitter voltage of Q_1 . This decrease in voltage is coupled through C_1 , thus decreasing the base-to-emitter voltage of Q_2 . Therefore, the collector current of Q_2 decreases, and

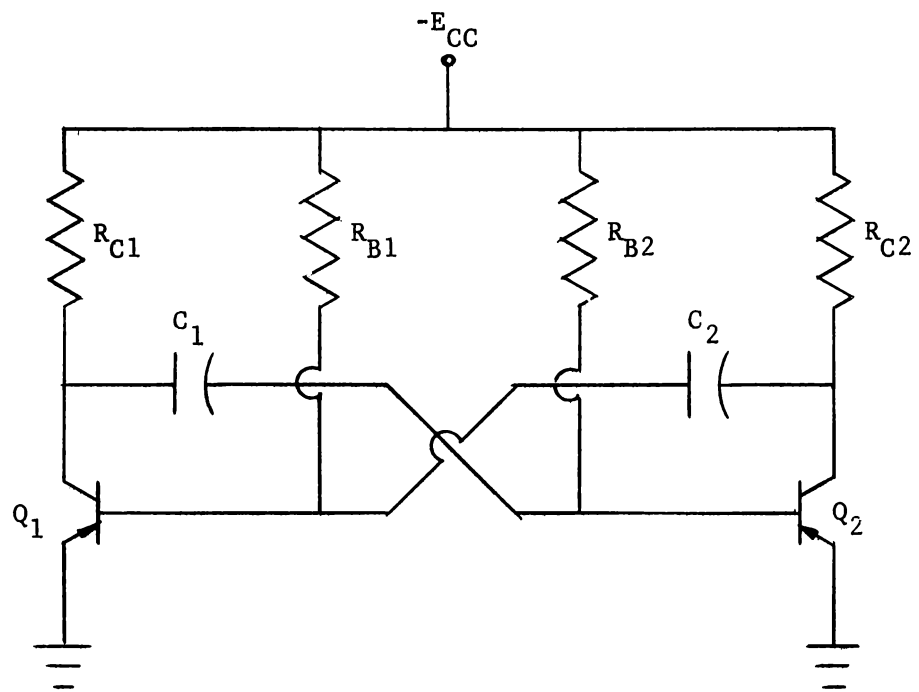


Figure 1. Circuit diagram of a transistor astable multivibrator.

through the coupling provided by C_2 , the base-to-emitter voltage of Q_1 increases further. Thus, a regenerative process occurs in which Q_1 is driven into saturation and Q_2 becomes nonconducting. Since this regenerative process is quite fast, the assumption is made that the time for the regenerative process is negligible with respect to the period of either quasi-stable state.

An equivalent circuit model for the period during which Q_1 is saturated and Q_2 is nonconducting is shown in Figure 2. To aid in simplifying the development of the circuit equations, the following symbols are used:

- V_F - Voltage toward which C is charging
- V_I - Initial capacitor voltage
- $V(T)$ - Voltage of the capacitor at which the transistor switches states
- V_T - Base-emitter voltage at which the transistor becomes conducting
- v_c - Collector-emitter instantaneous voltage
- v_b - Base-emitter instantaneous voltage
- SV_C - Collector-emitter saturation voltage
- SV_B - Base-emitter saturation voltage
- I_{CO} - Current of cutoff transistor

In addition, a numerical subscript following one of these symbols refers to a particular transistor or circuit element.

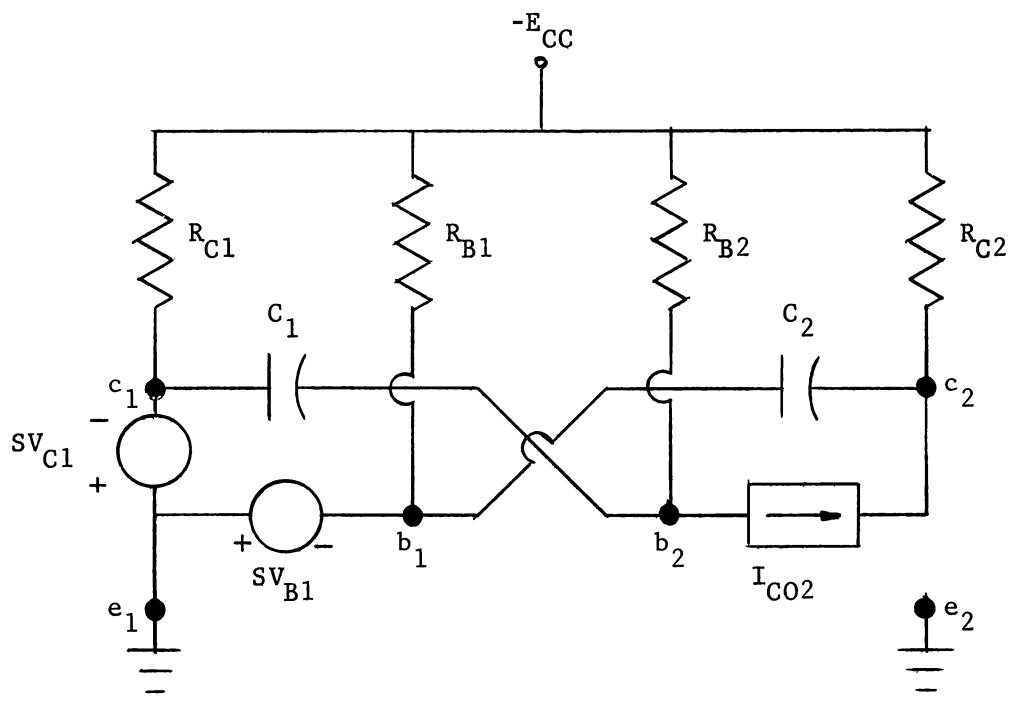


Figure 2. Circuit model of a transistor astable multivibrator with Q_1 saturated and Q_2 nonconducting.

With reference to Figure 2, page 7, as time increases, the voltage across C_1 changes which, therefore, changes v_{b2} . The equation for the voltage on C_1 with Q_1 saturated and Q_2 nonconducting, with the definition of $t = 0$ as the time Q_2 becomes nonconducting, is

$$v_1(t) = (V_{I1} - V_{F1})e^{-t/R_{B2}C_1} + V_{F1} \quad (1)$$

where e is the base for the natural logarithm. At the time the instantaneous capacitor voltage, $v_1(t)$, is equal to the capacitor voltage sufficient for Q_2 to conduct, regeneration occurs and the transistors change states. This time is defined as T_2 , and the corresponding capacitor voltage is $V_1(T_2)$. This period, T_2 , is then the total time Q_1 is saturated and Q_2 is nonconducting. Making the substitution $v_1(t) = V_1(T_2)$ at the time $t = T_2$ into Equation (1) gives

$$V_1(T_2) = (V_{I1} - V_{F1})e^{-T_2/R_{B2}C_1} + V_{F1} \quad (2)$$

Solving Equation (2) for the period during which Q_2 is nonconducting gives

$$T_2 = R_{B2}C_1 \ln \left[\frac{V_{F1} - V_{I1}}{V_{F1} - V_1(T_2)} \right] \quad (3)$$

The period, T_2 , given by Equation (3) is not useful until V_{F1} , V_{I1} , and $V_1(T_2)$ are known in terms of E_{CC} and the circuit and transistor parameters. The initial voltage on C_1 is determined by the conditions at $t = 0^-$, or when Q_1 is nonconducting but at the point of conduction and when Q_2 is saturated. This voltage is

$$V_{I1} = E_{CC} - SV_{B2} - I_{CO1}R_{C1} \quad (4)$$

The final voltage on C_1 is the voltage that C_1 would charge to if the switching of transistor states did not take place. This voltage is

$$V_{F1} = -E_{CC} - I_{CO2}R_{B2} + SV_{C1} \quad (5)$$

The voltage on C_1 where the transistors switch states is $V_1(T_2)$ and must be determined from the base-emitter voltage where Q_2 begins to conduct. Therefore, this capacitor voltage is

$$V_1(T_2) = -V_{T2} + SV_{C1} \quad (6)$$

Substitution of the equalities in Equations (4), (5), and (6) into Equation (3) gives

$$T_2 = R_{B2}C_1 \ln \left[\frac{2E_{CC} + I_{CO2}R_{B2} - SV_{C1} - SV_{B2} - I_{CO1}R_{C1}}{E_{CC} + I_{CO2}R_{B2} - V_{T2}} \right] \quad (7)$$

An expression for the period, T_1 , during which Q_2 is saturated and Q_1 is nonconducting can be obtained in a similar manner. The equation for T_1 is

$$T_1 = R_{B1}C_2 \ln \left[\frac{2E_{CC} + I_{CO1}R_{B1} - SV_{C2} - SV_{B1} - I_{CO2}R_{C2}}{E_{CC} + I_{CO1}R_{B1} - V_{T1}} \right] \quad (8)$$

A similar analysis of the time periods using the equivalent circuit shown in Figure 2, page 7, is given in the Motorola High-Speed Switching Transistor Handbook (2).

Equations (7) and (8) are the expressions for the time periods of the quasi-stable states of Q_1 and Q_2 . These equations in no way, however, demonstrate the voltage waveshapes at the collector and base of each transistor. These waveshapes are shown in Figure 3 and were

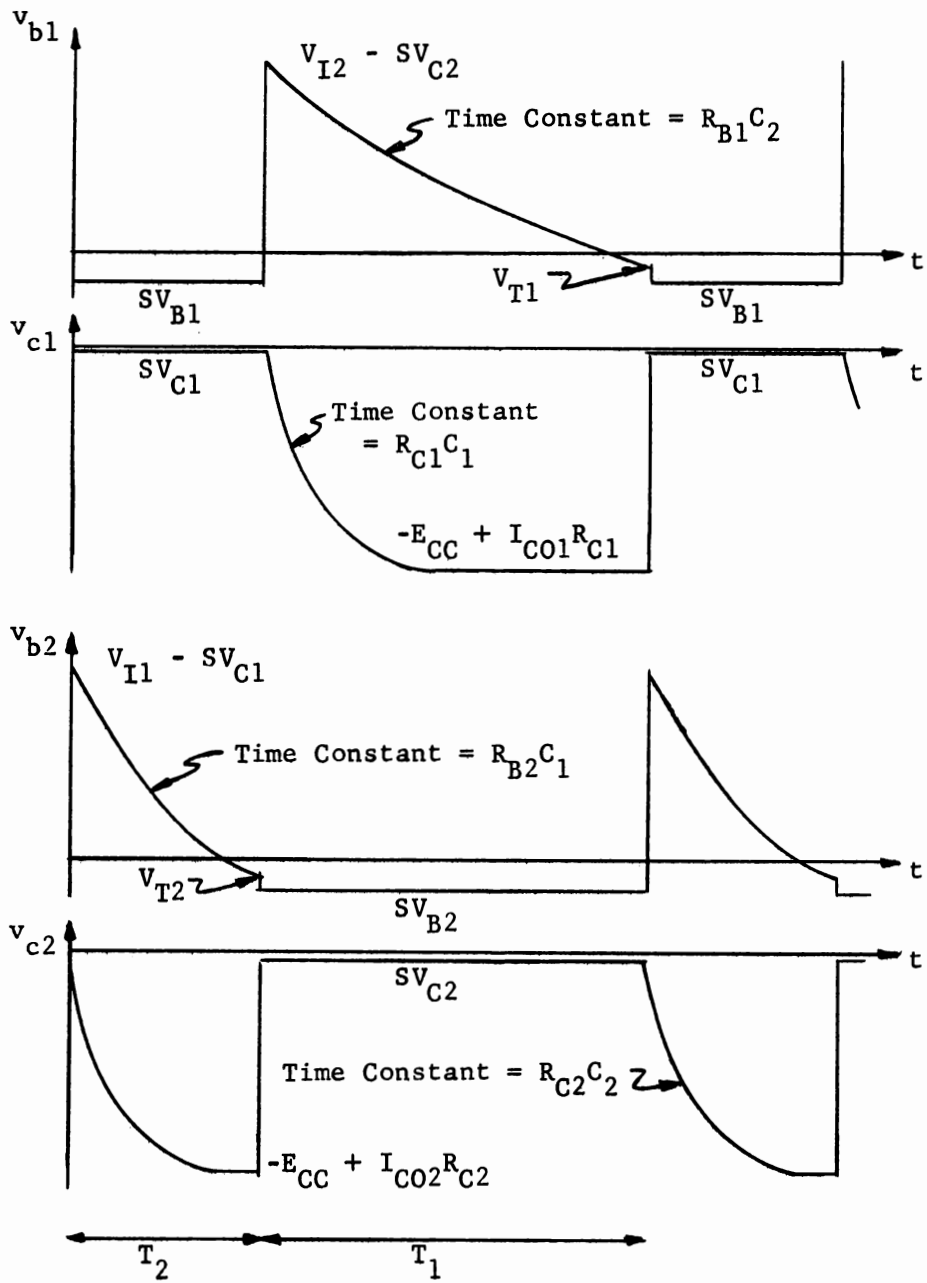


Figure 3. Voltage waveforms at the base and collector of each transistor as a function of time.

obtained by using Equation (2) and Figure 2, page 7. From Figure 3 the collector voltage waveshapes are nearly rectangular. The waveshapes become more nearly rectangular as the recovery rates become faster. For a good rectangular waveshape approximation, full recovery of the collector voltages was assumed in Figure 3, page 10. Not only does full recovery of the collector voltage more nearly approximate a rectangular waveshape; but, also, the collector voltage magnitude is largest in full recovery.

As indicated previously, the proper circuit elements must be used for the multivibrator to produce a free-running, rectangular voltage waveshape. The assumption of full recovery in the collector voltage waveshapes presents the first two limitations. The collector voltage of Q_2 for $0 \leq t \leq T_2$ is found from Figure 3, page 10. This voltage is

$$v_{c2}(t) = (-SV_{C2} + E_{CC} - I_{C02}R_{C2})e^{-t/R_{C2}C_2} - E_{CC} + I_{C02}R_{C2} \quad (9)$$

For full recovery, the transient portion, $(-SV_{C2} + E_{CC} - I_{C02}R_{C2}) \exp. (-t/R_{C2}C_2)$, must be zero. Absolute full recovery is not possible; but if $R_{C2}C_2$ is made one-fourth or less of the value of T_2 , $\exp. (-T_2/R_{C2}C_2)$ becomes two per cent or less. Therefore, recovery is within ninety-eight per cent of full recovery. Thus, in terms of circuit and transistor parameters, ninety-eight per cent recovery requires that $R_{C2}C_2$ be less than or equal to one-fourth T_2 . Substitution of Equation (7) into this requirement gives

$$4R_{C2}C_2 \leq R_{B2}C_1 \ln \left[\frac{2E_{CC} + I_{CO1}R_{B1} - SV_{C1} - SV_{B2} - I_{CO1}R_{C1}}{E_{CC} + I_{CO1}R_{B1} - V_{T1}} \right] . \quad (10)$$

From the collector voltage of Q_1 for Q_1 nonconducting a similar expression can be obtained. This inequality is

$$4R_{C1}C_1 \leq R_{B1}C_2 \ln \left[\frac{2E_{CC} + I_{CO2}R_{B2} - SV_{C2} - SV_{B1} - I_{CO2}R_{C2}}{E_{CC} + I_{CO2}R_{B2} - V_{T2}} \right] . \quad (11)$$

Another requirement is that each transistor must be saturated during the period in which the other transistor is nonconducting. In saturation the collector current becomes almost independent of base current, and this saturation occurs only in the region where the collector current is less than or just equal to h_{FE} times the base current.

Referring to Figure 2, page 7, the collector current for Q_1 saturated is the sum of the currents through R_{C1} and C_1 . The current through R_{C1} is

$$i_{R_{C1}} = \frac{E_{CC} - SV_{C1}}{R_{C1}} . \quad (12)$$

The current through a capacitance is the capacitance times the derivative of the capacitor voltage. Equation (1) gives the expression for the capacitance voltage. Taking the derivative of Equation (1), the current, i_1 , through C_1 with the sign changed to comply with the current direction is

$$i_1 = \frac{V_{I1} - V_{F1}}{R_{B2}} e^{-t/R_{B2}C_1} . \quad (13)$$

Substituting the expressions for V_{I1} and V_{F1} given by Equations (4) and (5) into Equation (13), i_1 becomes

$$i_1 = \frac{2E_{CC} - SV_{B2} - I_{CO1}R_{C1} + I_{CO2}R_{B2} - SV_{C1}}{R_{B2}} \left[e^{-t/R_{B2}C_1} \right]. \quad (14)$$

Therefore, the collector saturation current of Q_1 is

$$Si_{c1} = \frac{(2E_{CC} - SV_{B2} - I_{CO1}R_{C1} + I_{CO2}R_{B2} - SV_{C1})}{R_{B2}} \left[e^{-t/R_{B2}C_1} \right] + \frac{E_{CC} - SV_{C1}}{R_{C1}}. \quad (15)$$

The base saturation current of Q_1 is the sum of the currents through R_{B1} and C_2 . The current through R_{B1} is

$$i_{R_{B1}} = \frac{E_{CC} - SV_{B1}}{R_{B1}}. \quad (16)$$

The current through C_2 is

$$i_2 = \frac{E_{CC} + v_{c2}}{R_{C2}} - I_{CO2}. \quad (17)$$

Equation (9) relates v_{c2} to the circuit and transistor parameters, and substitution of this into Equation (17) gives

$$i_2 = \frac{(E_{CC} - I_{CO2}R_{C2} - SV_{C2})}{R_{C2}} \left[e^{-t/R_{C2}C_2} \right]. \quad (18)$$

Therefore, the base saturation current of Q_1 is

$$Si_{b1} = \frac{(E_{CC} - I_{CO2}R_{C2} - SV_{C2})}{R_{C2}} \left[e^{-t/R_{C2}C_2} \right] + \frac{E_{CC} - SV_{B1}}{R_{B1}}. \quad (19)$$

Substitution of Equations (15) and (19) into the requirement that the collector saturation current be less than h_{FE} times the base saturation current gives

$$\begin{aligned} & \frac{E_{CC} - SV_{C1}}{R_{C1}} + \frac{(2E_{CC} - SV_{B2} - I_{CO1}R_{C1} + I_{CO2}R_{B2} - SV_{C1})}{R_{B2}} \left[e^{-t/R_{B2}C_1} \right] \\ & < h_{FE1} \frac{E_{CC} - SV_{B1}}{R_{B1}} + \frac{h_{FE1}(E_{CC} - I_{CO2}R_{C2} - SV_{C2})}{R_{C2}} \left[e^{-t/R_{C2}C_2} \right]. \end{aligned} \quad (20)$$

For the saturation of Q_2 , an expression can be obtained in a similar manner. This inequality is

$$\begin{aligned} & \frac{E_{CC} - SV_{C2}}{R_{C2}} + \frac{(2E_{CC} - SV_{B1} - I_{CO2}R_{C2} + I_{CO1}R_{B1} - SV_{C2})}{R_{B1}} \left[e^{-t/R_{B1}C_2} \right] \\ & < h_{FE2} \frac{E_{CC} - SV_{B2}}{R_{B2}} + \frac{h_{FE2}(E_{CC} - I_{CO1}R_{C1} - SV_{C1})}{R_{C1}} \left[e^{-t/R_{C1}C_1} \right]. \end{aligned} \quad (21)$$

If the assumptions are made that the saturation voltages are much less than E_{CC} and that I_{CO1} and I_{CO2} have a negligible effect, Equations (10), (11), (20), and (21) can be rewritten as

$$4R_{C2}C_2 \leq R_{B2}C_1 \ln 2, \quad (22)$$

$$4R_{C1}C_1 \leq R_{B1}C_2 \ln 2, \quad (23)$$

$$\frac{1}{R_{C1}} + \frac{2}{R_{B2}} e^{-t/R_{B2}C_1} < \frac{h_{FE1}}{R_{B1}} + \frac{h_{FE1}}{R_{C2}} e^{-t/R_{C2}C_2}, \quad (24)$$

and

$$\frac{1}{R_{C2}} + \frac{2}{R_{B1}} e^{-t/R_{B1}C_2} < \frac{h_{FE2}}{R_{B2}} + \frac{h_{FE2}}{R_{C1}} e^{-t/R_{C1}C_1} . \quad (25)$$

The preceding four equations give four limitations on circuit and transistor parameters. These limitations and the limitations from the transistors chosen will be used to design a circuit where T_1 and/or T_2 varies with temperature.

Nothing so far has been determined about how the time periods are to vary with temperature. From the equations for T_1 and T_2 , many variations are possible. In the next chapter, the variables which are useful in making the periods a significant function of temperature will be determined.

CHAPTER III

VARIABLES IN THE PULSE-WIDTH EQUATION

The pulse-width expressions given by Equations (7) and (8) are functions of several variables. In this chapter, these variables will be studied with the objective of finding the variable that can produce the largest linear change in the pulse width as a function of temperature. These variables can be divided into two main categories, (1) the transistor parameters and (2) the circuit elements and E_{CC} . The transistor parameters are all certain functions of temperature for a particular transistor. The variables in the second category may be chosen to exhibit different temperature variations. Only the variables of T_2 will be examined; however, the same conclusions can be extended to the variables of T_1 .

The first category of variables contains I_{C01} , I_{C02} , SV_{C1} , SV_{B2} , and V_{T2} . For a particular transistor each of these variables is a specific function of temperature. In the cutoff region, the transistor currents, I_{C01} and I_{C02} , are exponential functions of temperature. The saturation base voltage, SV_{B2} , and the base threshold voltage, V_{T2} , are approximately linear functions of temperature. However, the collector saturation voltage, SV_{C1} , has different temperature characteristics for different transistors.

Several disadvantages may be observed in using the transistor parameters as the variables in the pulse-width equation. The first is

that all of the variables of one transistor change as the temperature of the transistor changes. Hence, a complicated temperature-dependent pulse-width function would be obtained. The second disadvantage is that the range of pulse-width variations obtained would be very small. This limitation is due to the logarithmic nature of the pulse-width function. The third disadvantage is that there is no systematic relationship for different transistors. For these reasons, the use of the transistor parameters as the dependent variables for the pulse width was eliminated.

The circuit variables in T_2 include E_{CC} , R_{B2} , C_1 , and R_{C1} . In examining these variables, the transistor parameters were assumed to be independent of the temperature variation of these variables. In addition, the transistor parameters were also assumed to be stabilized or compensated for a variation in the temperature of the transistor. In the Appendix, the effect of I_{CO} was shown to be negligible by choosing a transistor with a small I_{CO} value. Thus, only E_{CC} , R_{B2} , and C_1 need to be examined.

The first variable, E_{CC} , can be made large with respect to the other factors in the argument of the logarithm. In this case the expression for T_2 reduces to

$$T_2 = R_{B2} C_1 \ln 2 \quad . \quad (26)$$

If E_{CC} is dominant, the pulse width becomes independent of E_{CC} for any E_{CC} variation. However, if E_{CC} is not large with respect to the other factors, the pulse width becomes a complicated logarithmic function. In addition, only a very small range is available due to two factors,

(1) the function is logarithmic and (2) both the numerator and denominator of the argument of the logarithm have the same variation. Thus, E_{CC} is not a practical variable in the pulse-width equation.

If we assume that E_{CC} is constant and the transistor parameters are stabilized or compensated, Equation (7) becomes

$$T_2 = R_{B2} C_1 \ln K_1 \quad (27)$$

where K_1 is a constant. For a constant value of capacitance, the pulse width is then a linear function of R_{B2} and depends on temperature in the same way as R_{B2} . For a constant value of R_{B2} , the pulse width and C_1 also have a linear relationship. This linear relationship is not the only advantage in using R_{B2} or C_1 . Both are elements of the circuit and can be isolated from the remainder of the circuit. Therefore, the only variation with the temperature to be measured would be the variation of the isolated element. Another advantage is that R_{B2} or C_1 can be made a function of some other variable, such as voltage, which then is a function of temperature. This advantage makes the circuit very flexible in terms of different temperature variations. For these reasons, R_{B2} and C_1 are the most useful variables in obtaining a linear temperature-to-pulse width variation.

Although the same results may be obtained with a variation of either R_{B2} or C_1 , only R_{B2} will be considered because there are more suitable possibilities for R_{B2} as a function of temperature than for C_1 . The elimination of C_1 does not mean to imply, however, that situations will not be encountered where the variation of C_1 would not be advantageous.

In this chapter, the variables for a significant temperature relationship in the pulse-width equations were determined. The manner in which a change in the pulse widths affected the output waveform was not examined. In the next chapter, the variations in the output waveform will be examined, and the restrictions on these variations will be found.

CHAPTER IV

VARIATIONS IN OUTPUT WAVEFORMS

In the preceding discussion, only one time period, T_2 or the period when Q_2 is nonconducting, was considered. However, T_1 , or the period when Q_2 is conducting, can also vary. These two variations lead to two different possibilities for the output waveform. The first possibility is to make T_1 equal to T_2 , and let both periods vary at the same rate. In this case a variable-width rectangular output wave is obtained. The second possibility is to hold either T_1 or T_2 constant, and let the other period vary. In this case a constant-width pulse with a variable time between pulses is obtained. The object of this chapter is to examine and evaluate each output waveform possibility and to determine the range limitations of the waveform chosen.

From Equations (7) and (8), making T_1 equal to T_2 requires that transistors Q_1 and Q_2 have matched parameters. In addition, R_{B1} must equal R_{B2} and C_1 must equal C_2 . Further, with R_{B1} and R_{B2} as the variables, the rate of variation of these resistors with temperature must be the same. The remaining circuit and transistor parameter variations with temperature must be matched. Since this matching is difficult to obtain with any degree of accuracy and since there is no advantage for the purposes of this study in obtaining a variable-width square wave, the second possibility of only one time period variable is

the better method. From Figure 3, page 10, a constant-width pulse with variable pulse spacing is available at the collector of Q_2 if T_1 is held constant and T_2 is allowed to vary.

Examination of the second possibility with T_2 the variable period and T_1 constant gives the range of variation of T_2 . Since T_2 is the variable period, R_{B2} is the variable element; and the range of variation of R_{B2} is the same as the range of T_2 . The lower limit on R_{B2} was found from Equations (22) and (23). The inequality of Equation (23) can be replaced by an equality since all the elements of this equation are constants. Making this replacement gives

$$4R_{C1}C_1 = R_{B1}C_2 \ln 2 \quad . \quad (28)$$

Substituting the ratio of C_2 to C_1 from Equation (28) into Equation (22) and solving for R_{B2} gives

$$R_{B2} \geq \frac{16 R_{C1}R_{C2}}{R_{B1} (\ln 2)^2} \quad . \quad (29)$$

Equation (29) gives the lower limit for R_{B2} in terms of the other circuit parameters. The saturation of Q_2 appears to be the determining factor for the upper limit of R_{B2} . This saturation does determine the upper limit of R_{B2} if the transient currents are neglected as is usually done in multivibrator analysis. However, if the transients are included in the saturation of Q_2 , a larger range can be produced by adding an additional limitation. Equation (25) represents the relationship for Q_2 to saturate with the assumptions that the saturation voltages are much less than E_{CC} and that I_{CO1} and I_{CO2} have a negligible effect. If,

in Equation (25), $\exp. (-t/R_{B1}C_2)$ is made a maximum and $\exp. (-t/R_{C1}C_1)$ is made a minimum, the inequality holds for all time for which Equation (25) is applicable. At $t = 0$, $\exp. (-t/R_{B1}C_2)$ is a maximum and is equal to one. At the time Q_2 switches from saturation to nonconducting, $\exp. (-t/R_{C1}C_1)$ becomes a minimum since t is a maximum. This maximum time is at $t = T_1$ or from Equation (28) at $t = 4R_{C1}C_1$. Therefore, the minimum value of $\exp. (-t/R_{C1}C_1)$ is e^{-4} . Making these substitutions into Equation (25) gives

$$\frac{1}{R_{C2}} + \frac{1}{R_{B1}} < \frac{h_{FE2}}{R_{B2}} + \frac{h_{FE2}}{R_{C1}} e^{-4} . \quad (30)$$

If in Equation (30) the inequality is valid regardless of the value of R_{B2} , then the saturation of Q_2 becomes independent of R_{B2} . Equation (30) then becomes

$$\frac{1}{R_{C2}} + \frac{1}{R_{B1}} < \frac{h_{FE2}}{R_{C1}} e^{-4} . \quad (31)$$

Equation (31) is a further limitation on the circuit elements for the saturation of Q_2 to be independent of R_{B2} . Since the effect of I_{CO} was not considered in deriving the limitation given by Equation (31), this limitation is valid only to the point where the I_{CO} effect can be neglected.

Since R_{B2} can become very large, the limitations given by Equation (24) can be simplified further. With R_{B2} large, Equation (24) becomes

$$\frac{1}{R_{C1}} < \frac{h_{FE1}}{R_{B1}} + \frac{h_{FE1}}{R_{C2}} e^{-t/R_{C2}C_2} . \quad (32)$$

The inequality expressed by Equation (32) must be valid for all the period during which Q_1 is saturated. Therefore, it must be valid for the minimum value of $\exp. (-t/R_{C2}C_2)$ or the value at $t = T_2$ where t is a maximum. Since T_2 becomes large as R_{B2} increases, $\exp. (-t/R_{C2}C_2)$ approaches zero, and Equation (32) is simplified to

$$R_{B1} < h_{FE1} R_{C1} \quad . \quad (33)$$

Equation (33) is then a limitation on the circuit elements R_{B1} and R_{C1} .

Considering R_{B2} as the variable in the circuit shown in Figure 1, page 5, Equations (28), (29), (31), and (33) give the limitations on the circuit elements. Using these equations and the limitations imposed by the transistors chosen, circuit values can be found. Throughout the previous analyses, temperature stabilization and compensation of the transistor parameters and circuit elements has been assumed. To obtain this temperature independence, a modification of the circuit shown in Figure 1, page 5, must be introduced. Stabilization and compensation methods are treated in the following section. In addition, a circuit that satisfies each of the limitations is developed.

CHAPTER V

A TEMPERATURE COMPENSATED AND STABILIZED CIRCUIT

In many of the derivations, the assumption has been made that the circuit excluding R_{B2} was compensated or stabilized. Although R_{B2} can be isolated from the remainder of the circuit, the other circuit elements and parameters can vary with a change in circuit temperature. Thus, the remainder of the circuit must be compensated or stabilized for a circuit temperature variation. The development of this compensation and stabilization is the object of this section. Some of the effects of the circuit elements and parameters can be temperature stabilized by the proper choice of elements. Compensation for the other effects may be obtained by altering the original circuit shown in Figure 1, page 5.

If a transistor is chosen where I_{CO} is very low, thus making $I_{CO2}R_{B2}$ and $I_{CO1}R_{C1}$ negligible with respect to E_{CC} , then Equation (7) becomes

$$T_2 = R_{B2}C_1 \ln \left[\frac{2E_{CC} - SV_{C1} - SV_{B2}}{E_{CC} - V_{T2}} \right] . \quad (34)$$

In the Appendix, the I_{CO} effect of the 2N3640 transistor is shown to be negligible. Therefore, the proper choice of transistors eliminated three of the variables. In a similar manner, the choice of C_1 as a temperature stable capacitor eliminated any effect of a temperature

variation in the capacitor. The power supply variation was assumed to be negligible. The remaining possible variables were SV_{C1} , SV_{B2} , and V_{T2} .

For the 2N3640 the variation of SV_{C1} with temperature is very small and needs no compensation. However, SV_{B2} and V_{T2} are base-to-emitter voltages; and their changes are not negligible. Pierce (3) describes a method for temperature compensating the base-to-emitter voltage. In the circuit represented by Figure 4, this method is used. Also in Figure 4, circuit element values are included. These values were calculated from the requirements previously developed and from the restrictions placed by the transistors.

The calculation of these values can be made as follows: The turn-on and turn-off times of the transistor places the first limitation on the circuit elements. Since the time between pulses must be much greater than these transition times, T_1 and the minimum value for T_2 were chosen to be ten microseconds. The maximum collector to base voltage for the 2N3640 is twelve volts. To ensure that this voltage was not exceeded, E_{CC} and E_D were chosen to be six volts. To keep the base current of the transistor below the maximum specified for the 2N3640, the lower limit on R_{B2} was eight kilohms. Solving Equation (26) for C_1 and substituting the corresponding T_2 and R_{B2} values gave a value of approximately 2000 picofarads for C_1 .

Since in Equations (23) and (33) all of the elements are constants, the inequalities may be replaced by equalities. Solving Equation (23)

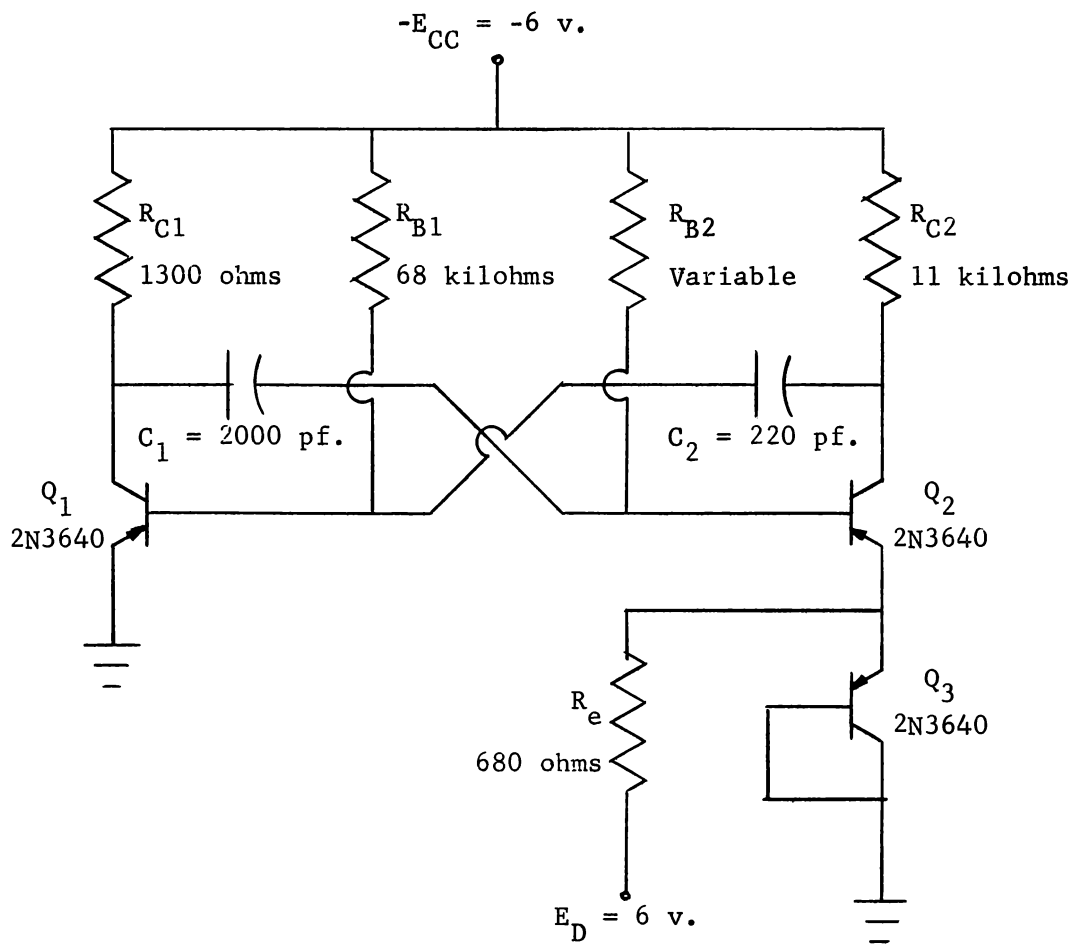


Figure 4. Circuit diagram of a temperature compensated and stabilized astable multivibrator.

for R_{C1} gave a value of approximately 1300 ohms for R_{C1} . A value of 68 kilohms for R_{B1} was found from the solution of Equation (33). From Equation (8), C_2 was found to be approximately 220 picofarads. If the minimum value for R_{B2} is used in Equation (11), the inequality can be replaced by an equality. Solving Equation (11) for R_{C2} gives 11 kilohms. The only limitation on R_e was that it have a value such that Q_3 is always forward-biased. Therefore, R_e was chosen to be 680 ohms. Substitution of the values for R_{C2} , R_{B1} , and R_{C1} into the inequality of Equation (31) showed that it was satisfied; therefore, R_{B2} is not limited by the saturation of Q_2 .

The addition of the voltage, V_D , or the base-to-emitter voltage of Q_3 shown in Figure 4, page 26, alters the T_2 expression given by Equation (34). The emitter of Q_2 is no longer at the same voltage as the emitter of Q_1 , but is increased by the value V_D . Therefore, the voltages, V_{I1} and $V_C(T_2)$, given by Equations (4) and (5) are increased by the value of V_D . Substituting these new values for V_{I1} and $V_C(T_2)$ into Equation (3) and neglecting the I_{C0} effects gives

$$T_2 = R_{B2} C_1 \ln \left[\frac{2E_{CC} - SV_{C1} - SV_{B2} + V_D}{E_{CC} - V_{T2} + V_D} \right] . \quad (35)$$

Since the changes in SV_{B2} , V_{T2} , and V_D with respect to temperature are almost equal, T_2 is then temperature compensated or stabilized for each of its variables except R_{B2} .

In this chapter, a circuit that theoretically generates pulses with a linear relationship between pulse spacing and R_{B2} was developed.

Also, temperature stabilization and compensation of the circuit excluding R_{B2} was developed. In the following chapter, experimental verifications of the theoretical predictions will be made.

CHAPTER VI

ANALYSIS OF PULSE SPACING WITH R_{B2} AS THE VARIABLE

The preceding developments predicted that R_{B2} in the circuit shown in Figure 4, page 26, could be varied from a minimum value of approximately eight kilohms to a maximum value that caused the effect of I_{C02} to be significant. In addition, T_2 could be expected to vary linearly over this range. The effect of the remainder of the circuit on T_2 was predicted to be independent of temperature variation. To substantiate these predictions, experimental results will be presented graphically together with theoretical calculations where applicable in this section.

To vary R_{B2} and to know the value of R_{B2} , resistor values having accuracies of one per cent were used. A Tektronix Type 555 oscilloscope was used to measure T_2 . The variation of T_2 as a function of R_{B2} is shown graphically in Figure 5. The calculation of the theoretical function is shown in the Appendix and is also shown graphically in Figure 5. A log-log plot was used in order that the entire range could be shown. The upper limit on R_{B2} , and hence T_2 , as shown in Figure 5 was not a result of the I_{C0} effect. This upper limit was due to the limitations of the oscilloscope measuring T_2 . The reason for the upper limit was that a ten microsecond pulse separated by about five milliseconds could not be synchronized on the oscilloscope to measure T_2 accurately.

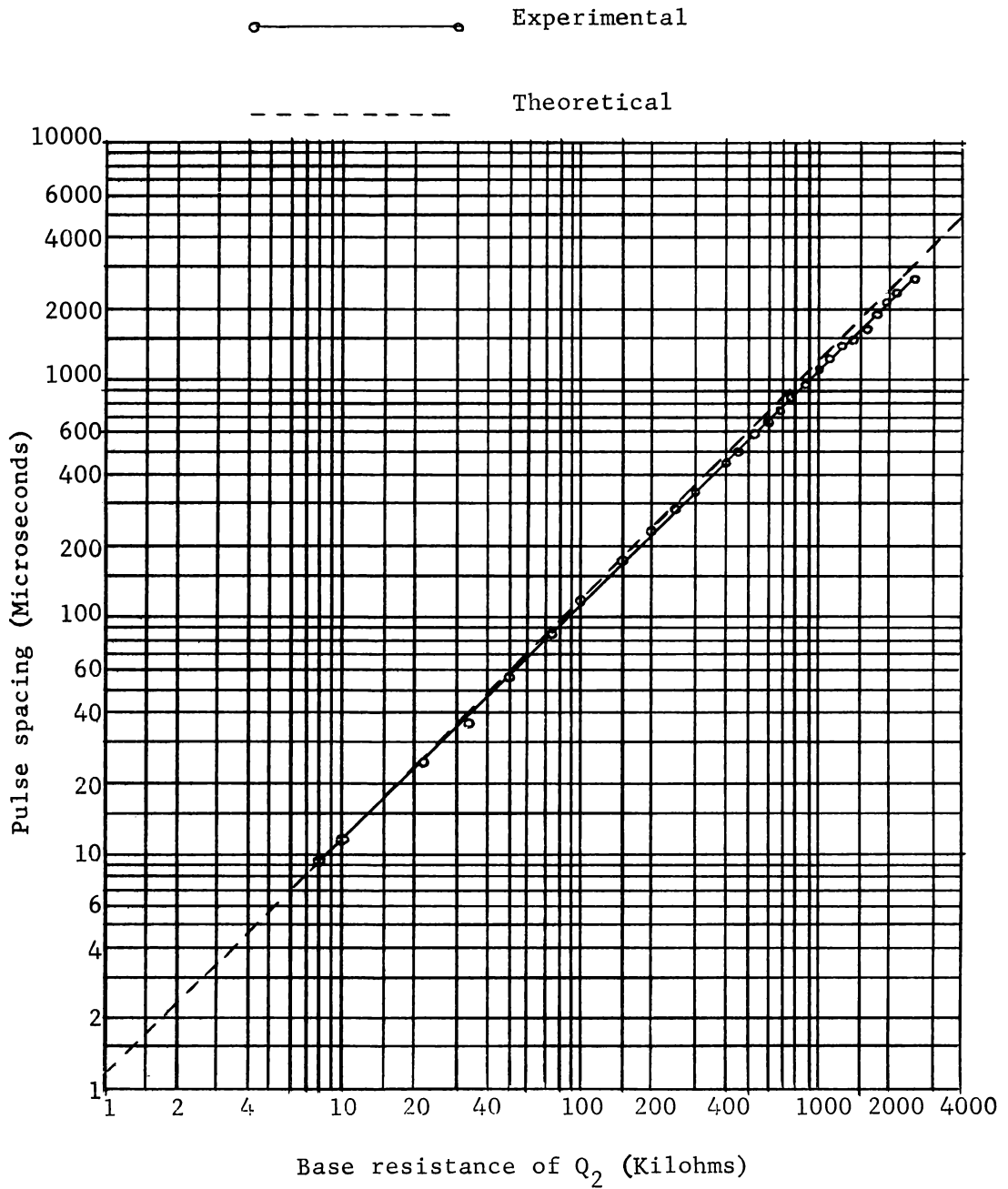


Figure 5. Pulse spacing as a function of R_{B2} .

A temperature-sensing resistor was then substituted for R_{B2} . The temperature of the resistor was varied and measured to show the relationship between T_2 and temperature. These results are shown in Figure 6. Since the resistor was actually an exponential function of temperature, a linear relationship between T_2 and temperature can only be approximated by small temperature variations. Two approximately linear ranges are shown in Figure 6.

To show the temperature independence of the circuit excluding R_{B2} , the temperature of this circuit was varied for different values of R_{B2} over the range shown by Figure 5, page 30. The time period, T_2 , was measured for these different temperatures. These results are shown in Figure 7.

From Figure 6, the range of T_2 was much smaller than the range possible. The reason for only a small portion of the range being used was because the temperature-sensing resistor varied only about 0.7 per cent per centigrade degree. To utilize more of the range available from this device, a modification of the circuit shown in Figure 1, page 5, will be introduced in the next section. Also included in the next section is the determination of the limits on the variable element and a comparison of theoretical and experimental results of the modified circuit.

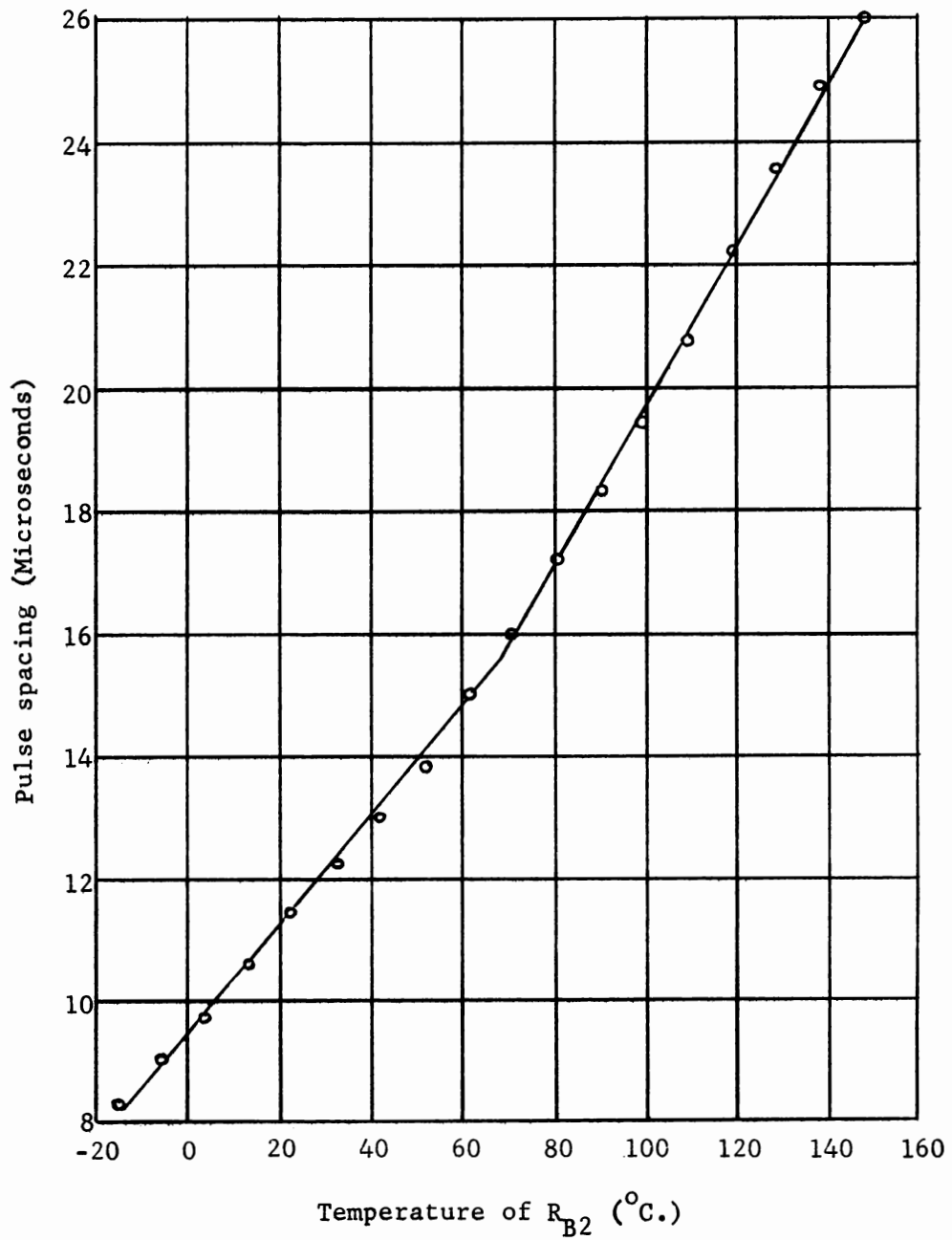


Figure 6. Pulse spacing as a function of the temperature of R_{B2} .

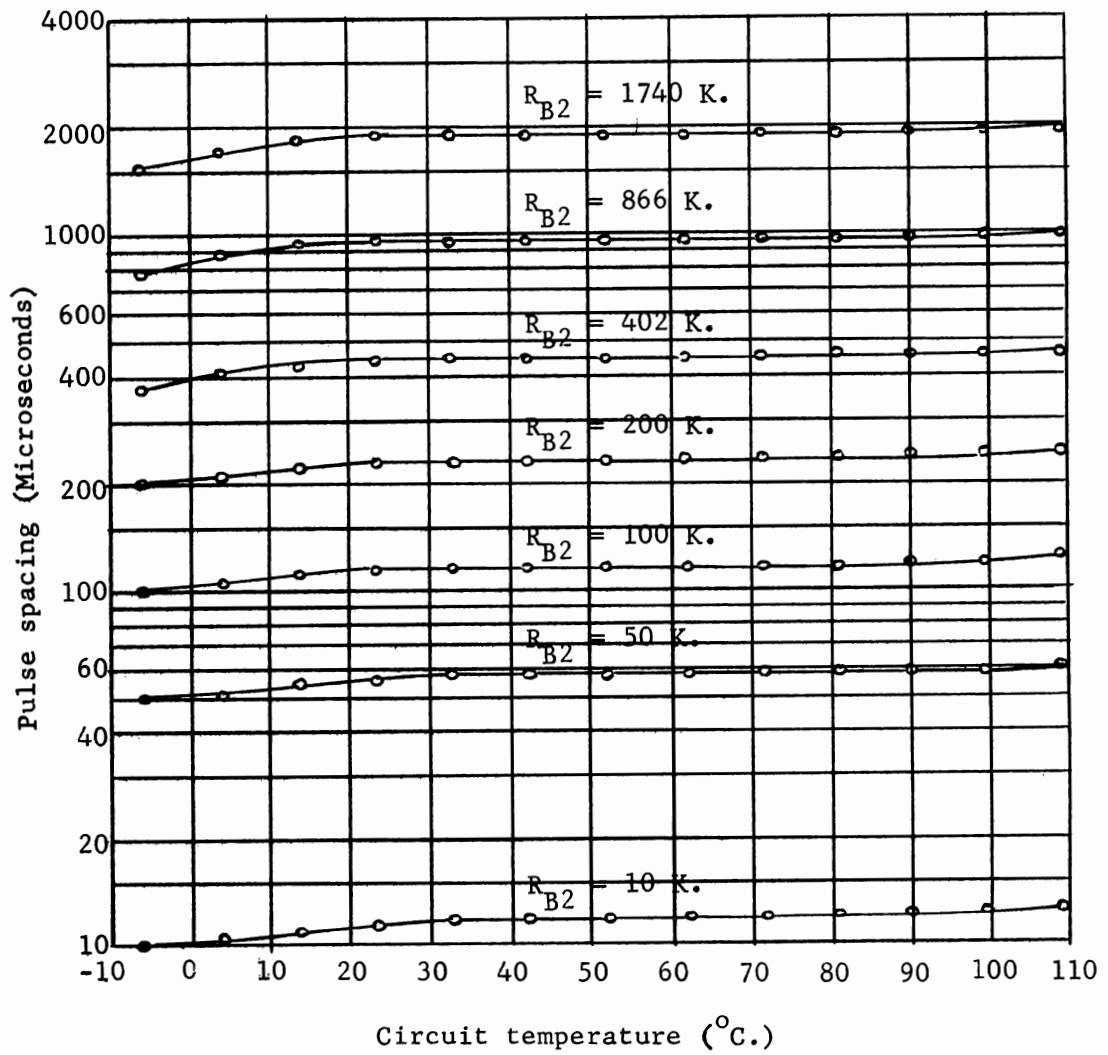


Figure 7. Pulse spacing as a function of circuit temperature.

CHAPTER VII

ANALYSIS OF THE OUTPUT SIGNAL WITH A CURRENT SOURCE

AS A REPLACEMENT FOR R_{B2}

The circuit shown in Figure 1, page 5, may be modified to provide a linear relationship between T_2 and the inverse of current by replacing R_{B2} with a current source. This relationship may be shown by analyzing the equivalent circuit model shown in Figure 8. This circuit model is for the state in which Q_1 is saturated and Q_2 is nonconducting. In the analysis the effect of I_{CO} is assumed to be negligible. With reference to Figure 8, the voltage at the base of Q_2 is

$$v_{b2} = -V_{I1} + SV_{C1} + \frac{1}{C_1} \int_0^t I_q dt \quad (36)$$

where $t = 0$ when Q_1 becomes conducting. The symbols used in this analysis have the same meaning as those in Chapter II. Equation (36) simplifies to

$$v_{b2} = -V_{I1} + SV_{C1} + \frac{I_q t}{C_1} \quad (37)$$

The initial voltage, V_{I1} , on C_1 is the voltage at $t = 0$ or when Q_1 begins conducting. This voltage is $E_{CC} - SV_{B2}$. At the time v_{b2} is equal to V_{T2} , the base voltage at which Q_2 begins to conduct, the transistors change states. The corresponding value of t , by definition, is T_2 . Making these substitutions into Equation (37) and solving for

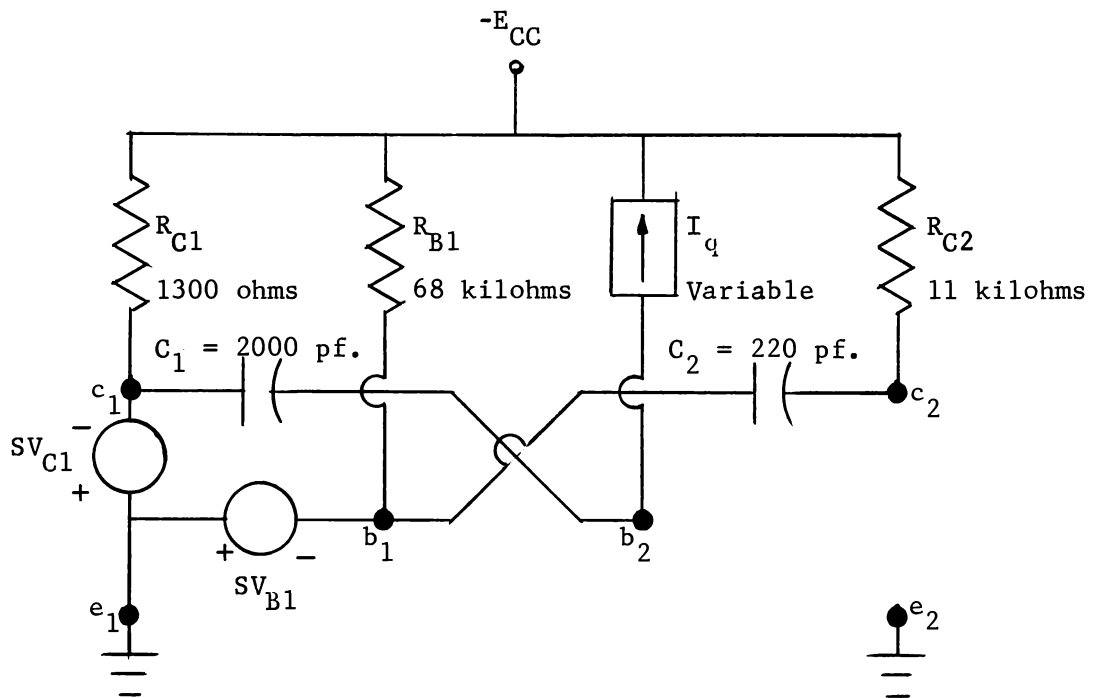


Figure 8. Circuit model of a transistor astable multivibrator with Q_1 saturated and Q_2 nonconducting with a current source as a replacement for R_{B2} .

T_2 gives

$$T_2 = \frac{C_1}{I_q} (E_{CC} + V_{T2} - SV_{B2} - SV_{C1}) \quad . \quad (38)$$

From Equation (38), T_2 is a linear function of I_q^{-1} .

The waveshapes of the voltage at the base and collector of each transistor are similar to those shown in Figure 3, page 10. The only change is in the base voltage of Q_2 for the time period, T_2 , and this is given by Equation (37). An analysis similar to that in Chapter IV shows that the circuit limitations given by Equations (28), (31), and (33) are exactly applicable for the case in which a current source replaces R_{B2} . Equation (31) placed a limitation on the circuit elements for the saturation of Q_2 to be independent of the value of R_{B2} . Similarly, the saturation of Q_2 is independent of I_q if the circuit elements satisfy equation (31). However, Equation (31) is valid only when the I_{CO} effect is negligible. Thus, the lower limit on I_q depends on the value of I_{CO} . The upper limit on I_q is obtained by substituting the expression for T_2 given by Equation (38) into Equation (10). Rearranging and solving for I_q gives

$$I_q \leq \frac{C_1}{4R_{C2}C_2} (E_{CC} + V_{T2} - SV_{B2} - SV_{C1}) \quad . \quad (39)$$

Since the limitations on the circuit values are the same, the circuit shown in Figure 4, page 26, is applicable with a current source as a replacement for R_{B2} . However, since V_{T2} and SV_{B2} are of the opposite sign in Equation (38), temperature compensation for base

voltage is not necessary. For test purposes the current source used was a simple transistor amplifier with a variable resistor in the emitter as shown in Figure 9. The 2N930 transistor was used for two reasons. The first reason was because an npn transistor was necessary for the correct current direction. The second reason was because the 2N930 operates well in the low-current region. Examination of the base voltage of Q_2 in Figure 3, page 10, and in Equation (36) shows that the proper bias voltage is maintained at the collector of the 2N930.

The current I_q was varied by changing the emitter resistor of the amplifier and was measured by a Hewlett-Packard Model 425A Micro Volt-Ammeter. The period T_2 was again measured by a Tektronix Type 555 oscilloscope. The results are shown in Figure 10. Also shown in Figure 10 is the graph of the theoretical function which is calculated in the Appendix.

Two constant-current devices that are predictable functions of temperature were used to obtain a digital signal that was dependent on temperature. The first device was a reverse-biased diode. Although the variation was exponential, the results of using the reversed-biased diode were included because of the large range of current available for a small temperature variation. The results of varying the temperature of the diode are shown in Figure 11.

The second constant-current source that was dependent on temperature is shown by the circuit diagram of Figure 12. From Equation

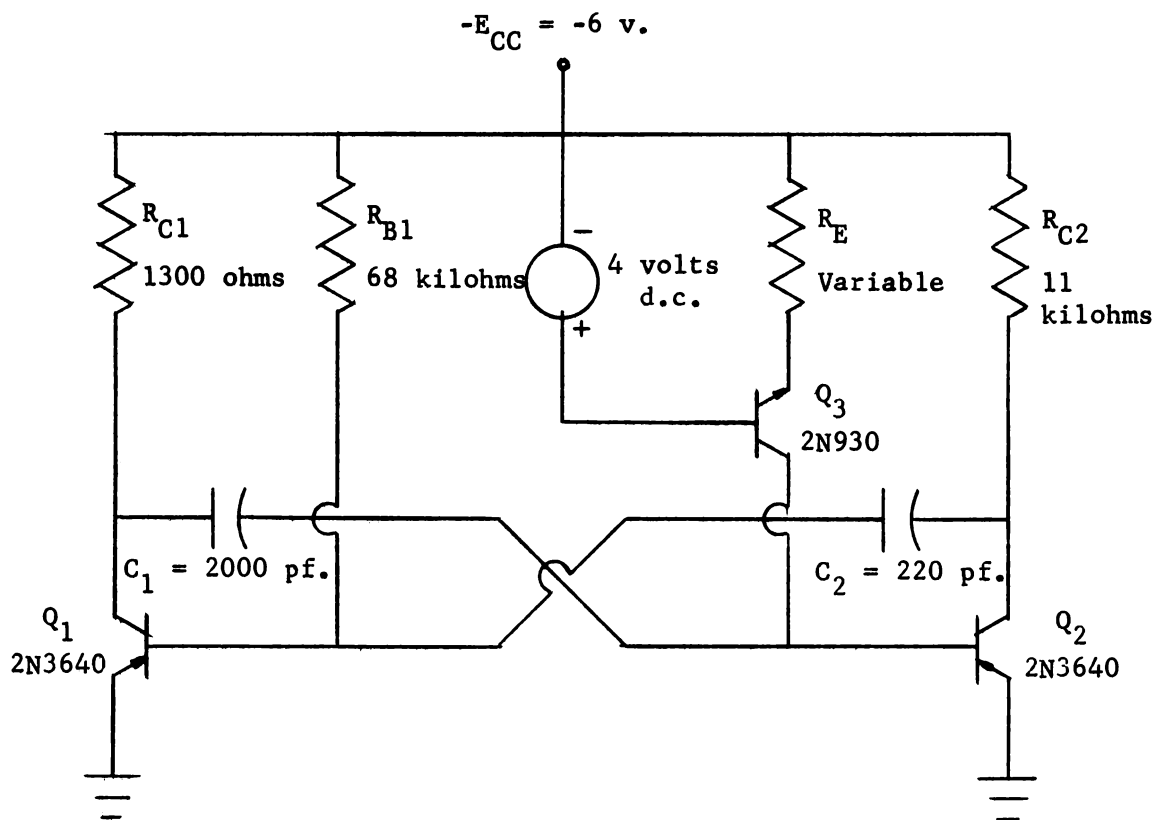


Figure 9. Circuit diagram of an astable multivibrator using a current source for R_{B2} .

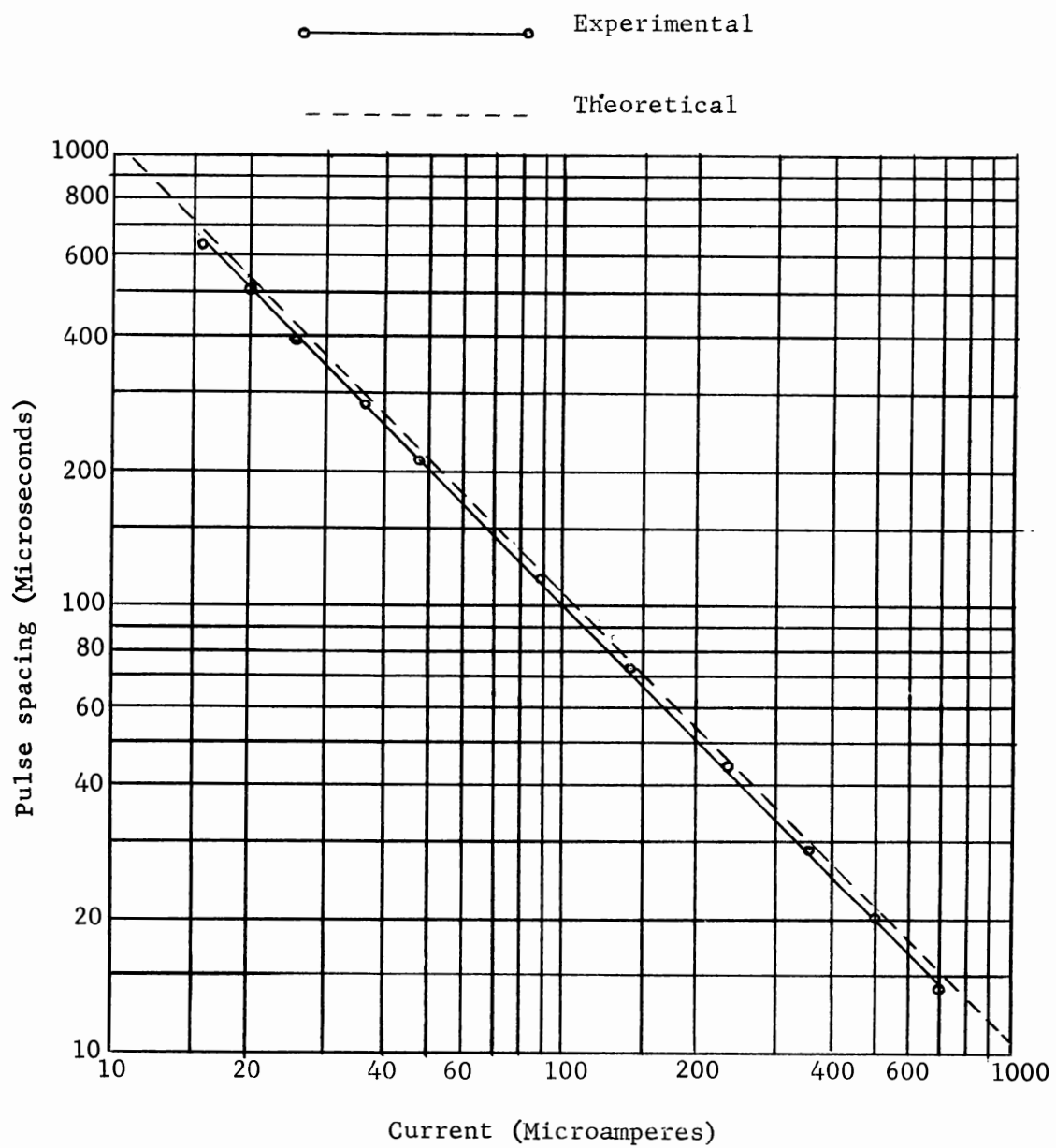


Figure 10. Pulse spacing as a function of the collector current of the current source.

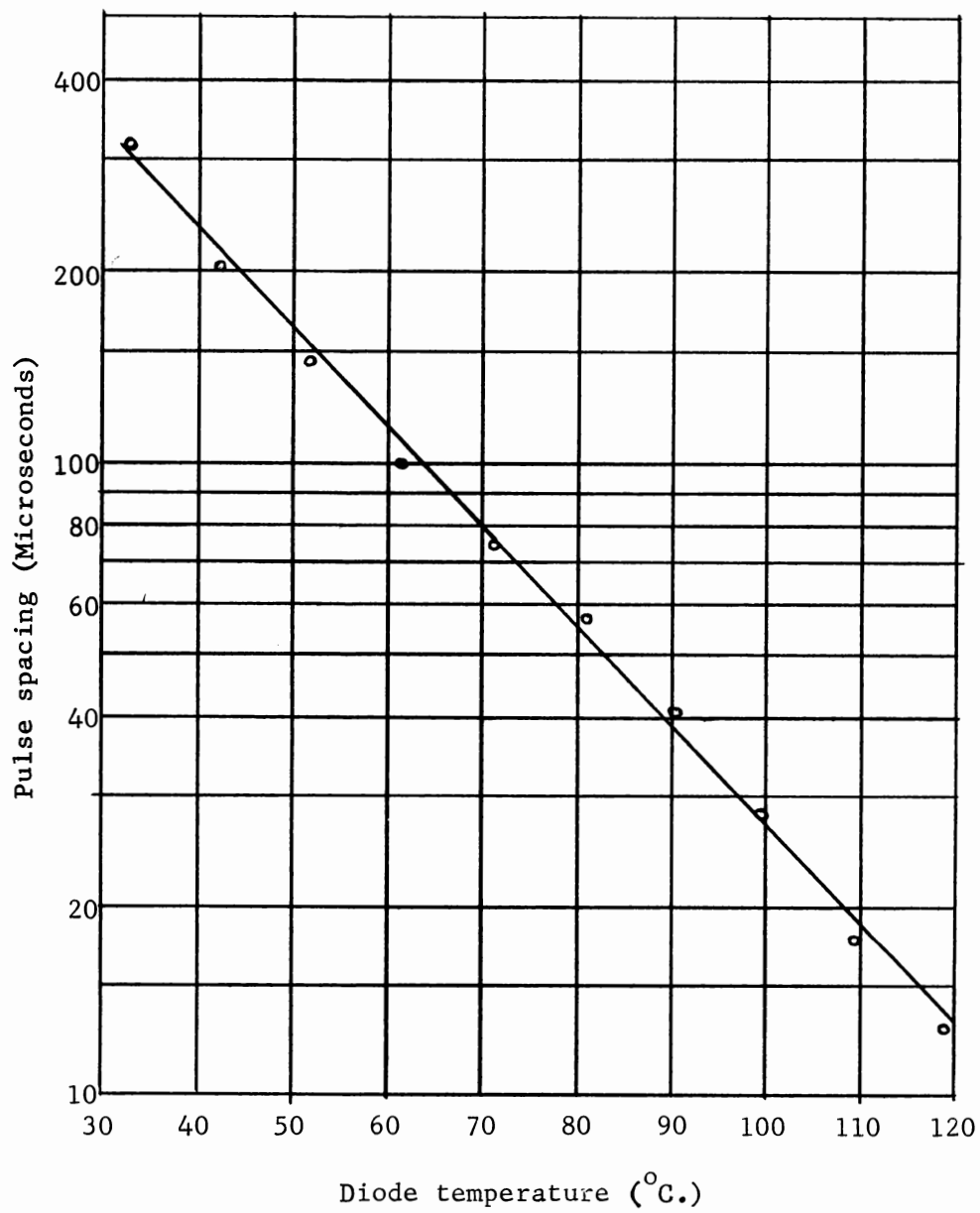


Figure 11. Pulse spacing as a function of diode temperature.

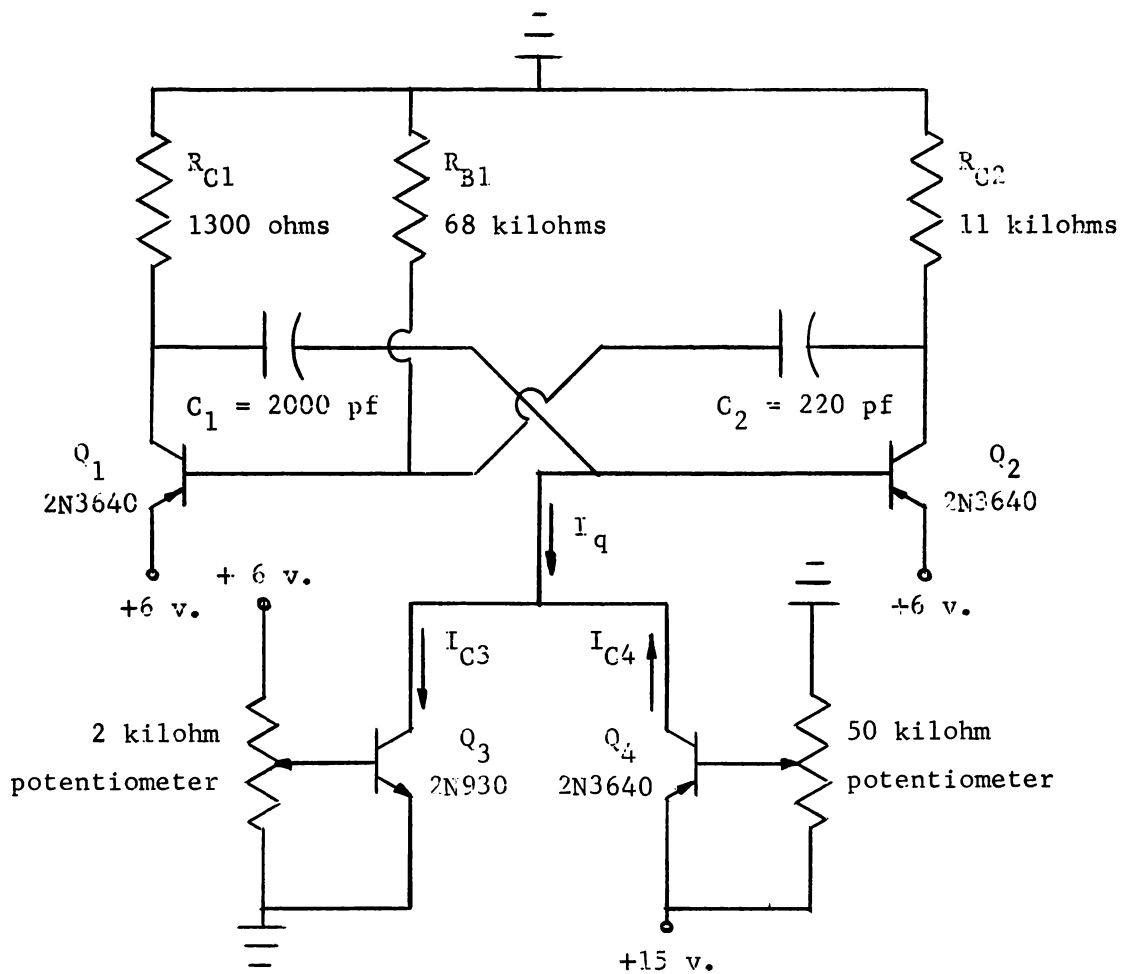


Figure 12. Circuit diagram of an astable multivibrator using a linear temperature-dependent current source.

(38), $1/T_2$ is a linear function of I_q . If I_q can be made a linear function of temperature, $1/T_2$ is then a linear function of temperature. The current I_q in Figure 12, page 41, is the difference between I_{C3} and I_{C4} . For currents above one milliampere, I_{C3} is approximately a linear function of the transistor temperature for a current range of about 1.0 ma. Since from Figure 10, page 39, I_q can vary from 0.02 ma. to 1.0 ma., the difference between I_{C3} and I_{C4} should be 0.02 ma. at the lowest temperature to be measured. If I_{C3} at this lowest temperature is 1.0 ma., I_{C3} increases linearly as the transistor temperature increases. Therefore, I_q increases linearly as the temperature of Q_3 increases. Different sensitivities can be obtained by adjusting the currents I_{C3} and I_{C4} at the lowest temperature.

The current I_{C4} is a reference current and must be stable. This current can be made very stable by using a differential amplifier. The conditions under which the amplifier operates determine the degree of stability necessary. Pierce (3) gives a good analysis of the differential amplifier and demonstrates how to predict the stability of the amplifier.

To demonstrate the linearity between $1/T_2$ and the temperature of Q_3 in Figure 12, page 41, an experimental test was made. In this test, I_{C3} was set at 1.0 ma. by varying the two-kilohm potentiometer. A two-kilohm potentiometer was used so that the effect of I_{B3} on V_{B3} was negligible. For I_q to be very small at the lowest temperature, I_{C4} was adjusted to be as close to 1.0 ma. as would be allowed for there to be

a signal. Since both I_{C3} and I_{C4} varied somewhat as v_{b2} varied, the lowest value of I_q possible was approximately 0.04 ma. Therefore, I_{C4} was set at 0.96 ma. at the lowest temperature. As the temperature of Q_3 increased, $1/T_2$ increased. The effect of a temperature increase on $1/T_2$ is shown in Figure 13. In making these measurements, a Tektronix Type 551 oscilloscope and a Hewlett-Packard Model 425A Micro Volt-Ammeter were used. With reference to Figure 13, the modification of the astable multivibrator provided a pulse generator in which the inverse of pulse spacing was linearly dependent on temperature over a large range for a small change in temperature.

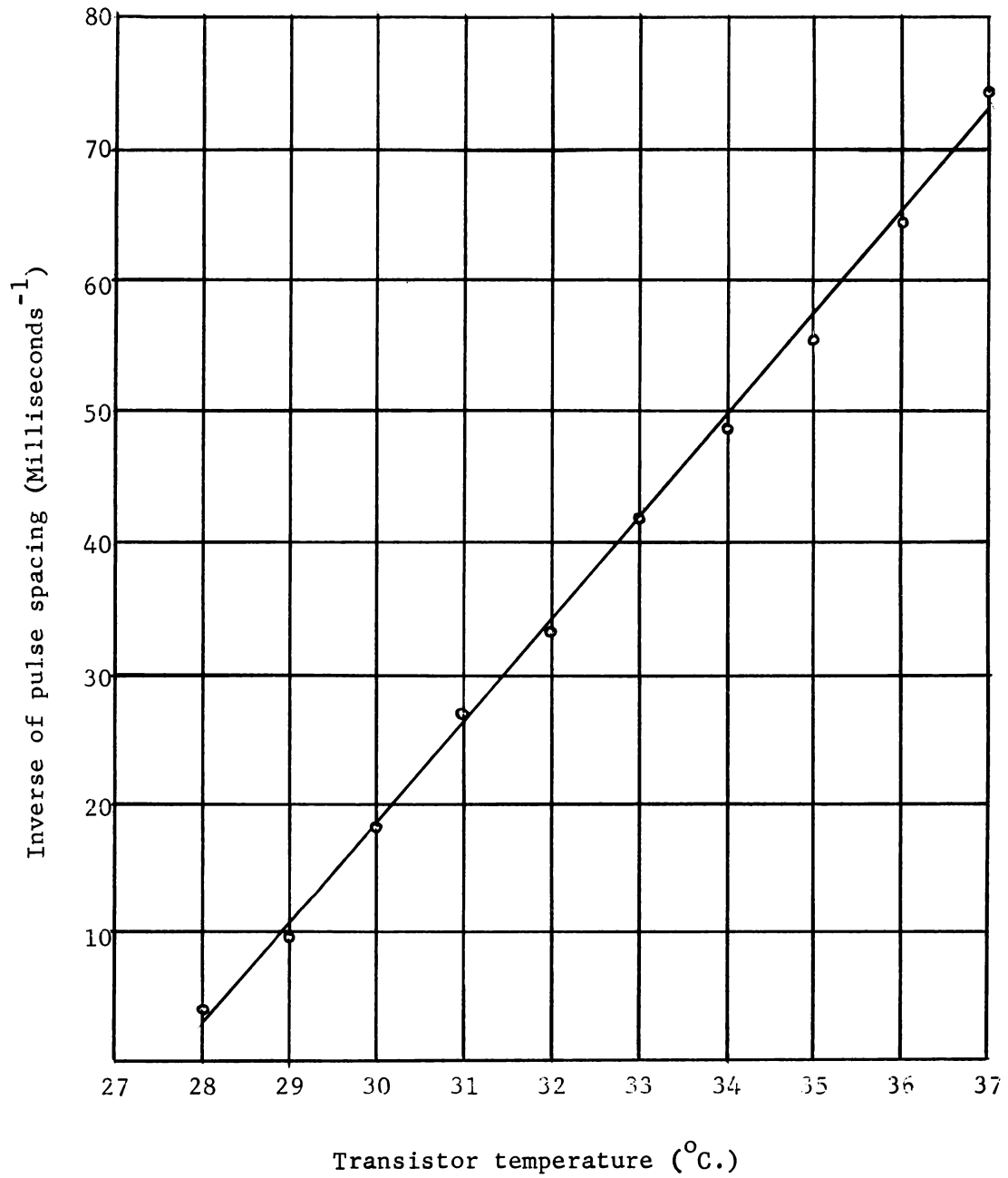


Figure 13. The inverse of pulse spacing as a function of transistor temperature.

CHAPTER VIII

SUMMARY

A collector-base, transistor, astable multivibrator was examined to determine the possibility of its use as a digital-signal generator that is linearly dependent on temperature. The operation of the multivibrator was described, the circuit equations and limitations were developed, and the most useful circuit variable and waveform were determined. The circuit, excluding the variable that was to change with the temperature to be measured, was temperature compensated and stabilized.

Examination of the equations for the pulse widths revealed that the pulse widths were a linear function of the base resistances, R_{B1} and R_{B2} . Because of matching problems, one pulse width was made constant, and the other was allowed to vary. This variation provided a constant-width pulse with a variable time between pulses at the collector of one of the transistors. This time between pulses was a linear function of R_{B2} .

Tests were made on the circuit to show that the theoretical results were physically valid. The results of these tests were presented graphically together with the theoretical results. A comparison of the experimental and theoretical results of T_2 as a function of R_{B2} showed that the maximum error was five per cent. The range of variation of T_2 was so large that the limitation on the experimental data was due to the measuring instruments and not to the circuit. The substitution of a

temperature-sensing resistor for R_{B2} produced a linear relationship between T_2 and temperature for small T_2 variations. The extreme range available, however, was of no use in the temperature-sensing resistor case because a large range of temperature affected resistance relatively little with respect to the desirable resistance variation.

The variation in temperature of the circuit excluding R_{B2} indicated that the circuit was very temperature stable. Over a temperature range of sixty centigrade degrees, T_2 varied approximately one per cent.

To utilize the available range of the circuit, a modification of the astable multivibrator was introduced. The base resistor, R_{B2} , was replaced by a current source. Analysis of the circuit showed that $1/T_2$ was a linear function of the current I_q from the current source. Tests made on the circuit verified the results of this analysis. Two temperature-dependent current sources were investigated in an effort to obtain a useful relationship between pulse spacing and temperature. A reverse-biased diode was used for the first current source. An exponential relationship between T_2 and temperature was obtained as expected since the reverse current of a diode is an exponential function of temperature. The second temperature-dependent current source was a transistor amplifier whose output current was linearly dependent on the transistor temperature. In this case, $1/T_2$ varied linearly over a large range for a small change in temperature.

If the pulse width T_1 is small compared with the pulse spacing T_2 , $1/T_2$ is approximately the pulse repetition rate. Therefore, the

circuit developed in this study could be used as a pulse generator with the pulse repetition rate linearly and sensitively dependent on temperature. The circuit could be further modified to obtain a linear relationship between $1/T_2$ and some other variable by providing a current source that was linearly dependent on that variable.

REFERENCES

LIST OF REFERENCES

1. Millman, Jacob, and Herbert Taub, Pulse, Digital, and Switching Waveforms, New York, New York: McGraw-Hill Book Company, 1965.
2. Roehr, William D. (ed.), Switching Transistor Handbook, Phoenix, Arizona: Motorola, Inc., 1963.
3. Pierce, John Franklin, Transistor Circuit Theory and Design, Columbus, Ohio: Charles E. Merrill Books, Inc., 1963.

APPENDIX

APPENDIX

CALCULATIONS OF THEORETICAL PULSE-SPACING FUNCTIONS

The calculations of the theoretical pulse-spacing functions given by Equations (35) and (38) will be made so that the experimental results may be compared to the theoretical result predicted. Equation (35) is derived from a modification of Equation (7) with the I_{CO} effect assumed negligible. In Equation (7) the $I_{CO_2}R_{B_2}$ term will be the larger of the I_{CO} effects, and if this effect can be shown to be negligible, then the other effects are also negligible. Experimentally, the maximum value of R_{B_2} was 2500 kilohms and the highest circuit temperature examined was 110 degrees Centigrade. The corresponding maximum value of I_{CO_2} was 40 nanoamps. Thus, the maximum effect of $I_{CO_2}R_{B_2}$ was about 0.10 volts. Since the $I_{CO_2}R_{B_2}$ effect is additive to both the numerator and denominator of the argument of the logarithm and since a value of E_{CC} equal to six volts dominates both the numerator and denominator, the I_{CO} effect is small and is negligible for lower temperatures or smaller values of R_{B_2} .

To measure the transistor parameters remaining in Equation (35), a Tektronix Type 555 oscilloscope was used. The voltages SV_{B_2} , SV_{C_1} , V_{T_2} , and V_D varied somewhat as R_{B_2} was changed. An average value was used in calculations containing these voltages. The following parameters were measured at 25 degrees Centigrade:

$$SV_{B2} = 1.0 \text{ volts} ,$$

$$SV_{C1} = 0.2 \text{ volts} ,$$

$$V_{T2} = 0.4 \text{ volts} ,$$

and

$$V_D = 0.8 \text{ volts} .$$

Substituting these values into Equation (35) gives

$$T_2 = R_{B2} \times 2000 \text{ pf.} \times \ln \frac{12 - 0.2 - 1.0 + 0.8}{6 - 0.4 + 0.8} .$$

This equation reduces to the T_2 versus R_{B2} function shown in Figure 6, page 32, and is

$$T_2 = 2 R_{B2} \ln \frac{11.6}{6.4} = 1.19 R_{B2}$$

where T_2 is in microseconds when R_{B2} is in kilohms.

The equation for T_2 as a function of the current, I_q , is given by Equation (38). Substitution of the measured parameters into this equation gives

$$T_2 = \frac{2000 \text{ pf.}}{I_q} (6 + 0.4 - 1.0 - 0.2) \text{ volts} .$$

This expression for T_2 simplifies to

$$T_2 = \frac{10.4 \times 10^3}{I_q}$$

where T_2 is in microseconds when I_q is in microamperes. This T_2 versus I_q function is shown in Figure 10, page 39.

